

THE STRUCTURAL EFFICIENCY OF TAPERED
STEEL SECTION WITH PERFORATION UNDER
LATERAL TORSIONAL BUCKLING BEHAVIOUR

LIM CHENG KUAN

SCHOOL OF CIVIL ENGINEERING
UNIVERSITI SAINS MALAYSIA
2018

**THE STRUCTURAL EFFICIENCY OF TAPERED STEEL SECTION
WITH PERFORATION UNDER LATERAL TORSIONAL BUCKLING
BEHAVIOUR**

By

LIM CHENG KUAN

This dissertation is submitted to

UNIVERSITI SAINS MALAYSIA

As partial fulfilment of requirement for the degree of

**BACHELOR OF ENGINEERING (HONS.)
(CIVIL ENGINEERING)**

School of Civil Engineering,
Universiti Sains Malaysia

June 2018



**SCHOOL OF CIVIL ENGINEERING
ACADEMIC SESSION 2017/2018**

**FINAL YEAR PROJECT EAA492/6
DISSERTATION ENDORSEMENT FORM**

Title: THE STRUCTURAL EFFICIENCY OF TAPERED STEEL SECTION
WITH PERFORATION UNDER LATERAL TORSIONAL BUCKLING
BEHAVIOUR

Name of Student: LIM CHENG KUAN

I hereby declare that all corrections and comments made by the supervisor(s) and examiner have been taken into consideration and rectified accordingly.

Signature:

Approved by:

(Signature of Supervisor)

Date :

Name of Supervisor :

Date :

Approved by:

(Signature of Examiner)

Name of Examiner :

Date :

ACKNOWLEDGEMENT

First and foremost, I would like to express my deepest gratitude to my supervisor Assoc. Prof. Dr. Fatimah De'nan, lecturer of Universiti Sains Malaysia for her invaluable guidance throughout my final year project. She had been sharing her knowledge and experience which helps me to complete this final year project. She had also sacrifices her time to teach me on how to use LUSAS software which I mainly used in this final year project to do the modelling.

I would also like to express my gratitude to my parents who has always been very supportive to me which enables me to complete my final year project. They have been very patient and caring for me throughout my research period. Without them, it would be difficult to complete this dissertation.

Last but not least, I would also like to express my gratitude to all my friends whom had given me support. I am also indebted to every individual whom had helped me throughout this research. I really appreciate all those comments and ideas that had helped me to prepare this dissertation. Thank you.

ABSTRAK

Rasuk tirus mempunyai keupayaan untuk menahan tekanan maksima di satu lokasi sementara tegasannya lebih rendah pada anggota lain dan oleh itu ia boleh mempunyai kecekapan struktur yang lebih tinggi berbanding dengan rasuk konvensional. Ia juga boleh memenuhi keperluan fungsinya di samping mengurangkan berat diri sendiri dan kos dalam pelbagai bidang kejuruteraan awam. Buka web dalam keratan keluli juga memudahkan penyepaduan perkhidmatan mekanikal dan elektrik seperti paip pengudaraan dan kabel elektrik dalam kedalaman struktur pancaran. Sebanyak 81 model dianalisis dengan menggunakan perisian LUSAS dan lima pembolehubah yang diasas adalah saiz pembukaan, bentuk pembukaan, susun atur pembukaan, nisbah tirus dan ketebalan bibir dan web. Momen lengkokan diperolehi dari keputusan di LUSAS manakala berat diri sendiri dan kecekapan struktur dikira secara manual. Dari hasilnya, saiz pembukaan $0.75D$ mempunyai kecekapan struktur tertinggi walaupun ia dapat menahan beban yang lebih kecil. Ini disebabkan oleh berat badannya yang lebih rendah berbanding saiz pembukaan yang lain. Bentuk pembukaan empat segi juga mempunyai kecekapan struktur tertinggi berbanding dengan pembukaan bulat dan pembukaan berlian. Peratusan peningkatan kecekapan struktur bentuk pembukaan empat segi dengan saiz $0.75D$ adalah yang tertinggi pada 3.07%. Bentuk pembukaan bulat dengan saiz $0.75D$ dengan susun atur pembukaan *Buka-Buka-Buka* mempunyai peningkatan peratusan tertinggi dalam kecekapan struktur iaitu 2.37%. Nisbah tirus sebanyak 0.3 adalah paling efisien dan peningkatan peratusan dalam kecekapan struktur adalah 114.36%. Ketebalan bibir 0.02m dan ketebalan web 0.015m mempunyai kecekapan struktur tertinggi pada 45.756 dan 29.171. Kesimpulannya, rasuk harus dapat menahan momentum besar dan mempunyai berat badan yang lebih rendah juga untuk memiliki kecekapan struktur yang tinggi.

ABSTRACT

Tapered beams have the ability to resist a maximum stress at a single location while the stresses are considerably lower at in the rest of the member and therefore it could have a higher structural efficiency compared to conventional beams. It could also satisfy functional requirements while reducing weight and cost in many fields of civil construction. Perforation in steel section also eases the integration of Mechanical and Electrical (M&E) services such as ventilation pipes and electrical cables within the structural depths of the beam. In this research, the structural efficiency of tapered steel section with perforation under lateral torsional buckling behaviour were investigated. A total of 81 models were analysed using LUSAS software and five variables that are being investigated are size of opening, shape of opening, opening layout, tapering ratio and flange and web thickness. Buckling moment is obtained from the results in LUSAS while self-weight and structural efficiency is calculated manually. From the results, opening size of 0.75D has the highest structural efficiency although it can withstand a smaller buckling load. This is due to its lower self-weight compared to other opening size. Square opening shape also has the highest structural efficiency compared to circular opening and diamond opening. The percentage increase in structural efficiency of square opening shape of 0.75D is the highest at 3.07%. Circular opening shape of 0.75D with Open-Open opening layout has the highest percentage increase in structural efficiency which is 2.37%. Tapering ratio of 0.3 is the most structurally efficient and the percentage increase in structural efficiency is 114.36%. The flange thickness of 0.02m and web thickness of 0.015m has the highest structural efficiency at 45.756 and 29.171 respectively. In conclusion, a beam should be able to resist large buckling moment and has a lower self-weight as well in order to has a high structural efficiency.

TABLE OF CONTENTS

ACKNOWLEDGEMENT.....	I
ABSTRAK	II
ABSTRACT.....	III
TABLE OF CONTENTS	IV
LIST OF FIGURES	VI
LIST OF TABLES	IX
CHAPTER 1 INTRODUCTION	1
1.1 Background	1
1.2 Structural Efficiency	2
1.3 Tapered Steel Section.....	2
1.4 Perforation in Steel Section.....	3
1.5 Problem Statement	4
1.6 Objectives.....	5
1.7 Scope of study	6
CHAPTER 2 LITERATURE REVIEW.....	7
2.1 Tapered Steel Section.....	7
2.2 Perforated Steel Section	13
2.3 Structural Efficiency	19
2.4 Lateral Torsional Buckling.....	24
2.5 Summary	31
CHAPTER 3 METHODOLOGY	33
3.1 Introduction	33

3.2	Finite Element Analysis by LUSAS	35
3.3	Model Geometry	37
3.4	Model Attributes	37
3.5	Convergence Study	41
3.6	Terminologies Used for the Section.....	43
3.7	Result Verification of LUSAS Software.....	44
CHAPTER 4 RESULTS AND DISCUSSION.....		48
4.1	Introduction	48
4.2	Eigenvalue Buckling Analysis	48
4.2.1	Effect of Different Opening Size of Perforation.....	50
4.2.2	Effect of Different Opening Shape of Perforation.....	54
4.2.3	Effect of Different Opening Layout.....	60
4.2.4	Effect of Different Tapering Ratio.....	65
4.2.5	Effect of Different Flange Thickness.....	69
4.2.6	Effect of Different Web Thickness	74
4.3	Failure Pattern for Tapered Steel Section with Perforation and without Perforation.....	77
4.4	Summary	80
CHAPTER 5 CONCLUSIONS AND RECOMMENDATIONS		81
5.1	Conclusion	83
5.2	Recommendation for Future Research	85
REFERENCES.....		86
APPENDICES		

LIST OF FIGURES

Figure 1.1 : Geometry of Typical Web Tapered I-Beam (Polyzois & Raftoyiannis, 1998)	3
Figure 1.2 : Shapes of perforation (Hasan et al., 2017)	4
Figure 2.1 : A web tapered tee-section cantilever beam subject to a uniformly distributed load and a concentrated load at its free end (Yuan et al., 2013)	12
Figure 2.2 : Perforated section force distribution (Rodrigues et al., 2014)	18
Figure 2.3 : Buckling moment resistance versus flange thickness for TriWP with diamond perforation shape and perforation size of 0.4D in Layout 3 (Hasan et al., 2017)	23
Figure 2.4 : Buckling moment resistance versus web thickness for TriWP with diamond perforation shape and perforation size of 0.4D in Layout 3 (Hasan et al., 2017)	23
Figure 2.5 : Mesh view of the considered web-tapered beam $L=6m$, ($\alpha = 0.4$) (Benyamina et al., 2013)	25
Figure 2.6 : A simply supported tapered I-beam with doubly symmetric cross section (Benyamina et al., 2013)	25
Figure 2.7 : LTB of cellular beam shown by FE analysis (Sehwail, 2013)	28
Figure 2.8 : LTB of cellular beams (Sehwail, 2013)	28
Figure 3.1: Flow chart of methodology	34
Figure 3.2: Flow chart of modelling by using LUSAS software	36
Figure 3.3 : Triangular thin shell for TSL6 and quadrilateral thin shell QSL8	38
Figure 3.4 : Material Property used in LUSAS software for modelling	39
Figure 3.5 : Structural support used in LUSAS software for modelling	40
Figure 3.6 : Graph of maximum displacement against number of element	42

Figure 3.7 : Visualisation of distance to perforation, maximum and minimum depth of the beam.....	43
Figure 3.8 : Open-Open-Open (OOO) Layout.....	44
Figure 3.9 : Open-Close-Open (OCO) Layout	44
Figure 3.10 : Close-Open-Close (COC) Layout	44
Figure 3.11 : Uniform I-section from LUSAS.....	44
Figure 3.12 : I-section Beam.....	45
Figure 3.13 : Displacement Result from LUSAS	46
Figure 4.1 : Results of eigenvalue 1.....	49
Figure 4.2 : Results of eigenvalue 2.....	49
Figure 4.3 : Results of eigenvalue 3.....	49
Figure 4.4 : Tapered steel section with 0.3D web opening.....	50
Figure 4.5 : Tapered steel section with 0.75D web opening.....	50
Figure 4.6 : Graph of Buckling Moment against Opening Size	54
Figure 4.7 : Graph of Structural Efficiency against Opening Size	54
Figure 4.8 : Circular Opening Shape	55
Figure 4.9 : Square Opening Shape	55
Figure 4.10 : Diamond Opening Shape.....	55
Figure 4.11 : Graph of Buckling Moment against Opening Size for three different opening shapes	60
Figure 4.12 : Graph of Structural Efficiency against Opening Size for three different opening shapes	60
Figure 4.13 : Open-Open-Open (OOO) Layout.....	61
Figure 4.14 : Open-Close-Open (OCO) Layout	61
Figure 4.15 : Close-Open-Close (COC) Layout	61

Figure 4.16 : Graph of Buckling Moment against Opening Size for different opening layout.....	65
Figure 4.17 : Graph of Structural Efficiency against Opening Size for different opening layout.....	65
Figure 4.18 : Tapered steel section with 0.3 tapering ratio.....	66
Figure 4.19 : Tapered steel section with 0.75 tapering ratio.....	66
Figure 4.20 : Graph of Buckling Moment against Tapering Ratio	69
Figure 4.21 : Graph of Structural Efficiency against Tapering Ratio.....	69
Figure 4.22 : Tapered steel section with 0.02m flange thickness	70
Figure 4.23 : Graph of Buckling Moment against Flange Thickness	73
Figure 4.24 : Graph of Structural Efficiency against Flange Thickness.....	73
Figure 4.25 : Tapered steel section with 0.015m web thickness	74
Figure 4.26 : Graph of Buckling Moment against Web Thickness	77
Figure 4.27 : Graph of Structural Efficiency against Web Thickness	77
Figure 4.28 : Displacement contour for tapered steel section without perforation (Max Displacement = 5.21mm).....	78
Figure 4.29 : Displacement contour of tapered steel section with perforation (Max Displacement : 5.43mm).....	79
Figure 4.30 : Deformed mesh for tapered steel section without perforation	80
Figure 4.31 : Deformed mesh for tapered steel section with perforation	80
Figure 4.32 :Most efficient tapered steel section with perforation	82

LIST OF TABLES

Table 2.1 : I-cantilever web tapered beam (Asgarian et al., 2013).....	9
Table 2.2 : Simply supported web tapered I-section under distributed load (Asgarian et al., 2013)	10
Table 2.3 : Self-weight of TriWP with perforation for Layout 3 (Hasan et al., 2017) ..	19
Table 2.4 : Percentage difference of weight reduction of TriWP with perforation for Layout 3 (Hasan et al., 2017).....	20
Table 2.5 : Buckling load of TriWP with perforation (Hasan et al., 2017)	21
Table 2.6 : Structural efficiency of TriWP with perforation (Hasan et al., 2017)	22
Table 2.7 : Simply supported web tapered I-section under a distributed load (Figure 2.5) on the top flange $e_z = 0.3$ m ,buckling moment comparisons and relative errors (Benyamina et al., 2013).....	26
Table 2.8 : Buckling moment, M_b for span 3.5m and ratio of tapering 0.5 with opening size varies from 0.2D to 0.7D (Azar et al., 2015).....	30
Table 2.9 : Buckling moment, M_b for span 5.5m and tapering ratio 0.5 with opening size varies from 0.2D to 0.7D (Azar et al., 2015)	30
Table 3.1 : Dimensional Properties of Sample Models	41
Table 3.2 : Data of maximum displacement of I-beam model	42
Table 3.3 : Table of section properties.....	45
Table 4.1 : Properties of the model.....	51
Table 4.2 : Buckling moment, M_b and Structural Efficiency for 5.5m span and ratio of tapering of 0.5 with circular opening size varies from 0.3D to 0.75D	53
Table 4.3 : Properties of the model.....	56
Table 4.4 : Buckling moment, M_b and Structural Efficiency for 5.5m span and ratio of tapering of 0.5 with square opening size varies from 0.3D to 0.75D	58

Table 4.5 : Buckling moment, M_b and Structural Efficiency for 5.5m span and ratio of tapering of 0.5 with diamond opening size varies from 0.3D to 0.75D.....	59
Table 4.6 : Properties of the model.....	62
Table 4.7 : Buckling moment, M_b and Structural Efficiency for 5.5m span and ratio of tapering of 0.5 with circle opening size varies from 0.3D to 0.75D with different opening layout.....	63
Table 4.8 : Properties of the model.....	67
Table 4.9 : Buckling moment, M_b and Structural Efficiency for 5.5m span with 0.5D circular opening size with Open-Open-Open (OOO) opening layout and tapering ratio varies from 0.3 to 0.75	68
Table 4.10 : Properties of the model.....	70
Table 4.11 : Buckling moment, M_b and Structural Efficiency for 5.5m span with 0.5D circular opening size with Open-Open-Open (OOO) opening layout and flange thickness varies from 0.01m to 0.02m.....	72
Table 4.12 : Properties of the model.....	75
Table 4.13 : Buckling moment, M_b and Structural Efficiency for 5.5m span with 0.5D circular opening size with Open-Open-Open (OOO) opening layout and web thickness varies from 0.006m to 0.015m.....	76
Table 5.1 : Properties of tapered steel section with perforation with the highest structural efficiency.....	84

CHAPTER 1

INTRODUCTION

1.1 Background

Structural steel is used widely by structural engineers all around the world. Its usage increased in recent decades especially in those developed countries due to its ease of erection. Besides that, structural steel could also be recycled and thus it is environmental friendly. More types of steel sections were created as the technology of steel structure progress to obtain sections that has a better mechanical properties while at the same time satisfying the architectural needs (Sehwail, 2013).

As cost has always been an important factor to be consider during construction, choosing structural steel in your project will help to reduce the overall costs and enhance its value. It could result in general condition savings as steel framing can be constructed in a faster manner and this will reduce the labour cost that is required. Structural steel is also sleek and dynamic material that could form aesthetically pleasing structures. The steel industry has also reduces the emissions of greenhouse gases significantly due to its high recycled content and recycling rate exceed those of any other construction material. To be in line with the sustainable development goals, more building owners, architects, engineers and contractors are realizing the benefits of using structural steel as a means of meeting sustainable design and construction goals (American Institute of Steel Construction, 2018).

1.2 Structural Efficiency

Structural efficiency is measured in terms of weight of material which should be provided to carry a given amount of load (Hasan et al., 2017). It is possible to specify precisely the level of structural efficiency based on two main parameters which are the load carrying capacity and self-weight of the section. A structure is said to have a high efficiency if it has a higher load carrying capacity while it has a low self-weight. The concept basically is to reduce the self-weight as much as possible without compromising the load carrying capacity of the steel section. The self-weight of the steel section is dependent on the shapes of structural elements and also the shape and size of perforation (Hasan et al., 2017).

In the case of a beam, the structural efficiency of a beam with a particular cross-sectional shape decreases as the length of the span increases. Therefore, different types of efficient shapes of cross section have to be utilized to maintain a constant level of efficiency for different span length (Macdonald, 2007).

1.3 Tapered Steel Section

The conventional I-beams are frequently used to carry bending moments due to their superior moment of inertia to area ratio. If the bending moment is uniform throughout the whole beam, then a uniform cross section I-beam is the most efficient. However in most cases, the bending moment will not be uniform throughout the beam but it will varies linearly, therefore the beam cross-section should also varies linearly (Thomas, 2014).

Tapered beams have the ability to resist a maximum stress at a single location while the stresses are considerably lower at in the rest of the member. This will help to save materials and also the cost of construction (Polyzois & Raftoyiannis, 1998). In this study, focus will be given on web tapered steel section instead of flange tapered steel section. Figure 1.1 shows the geometry of a typical web tapered I-beam.

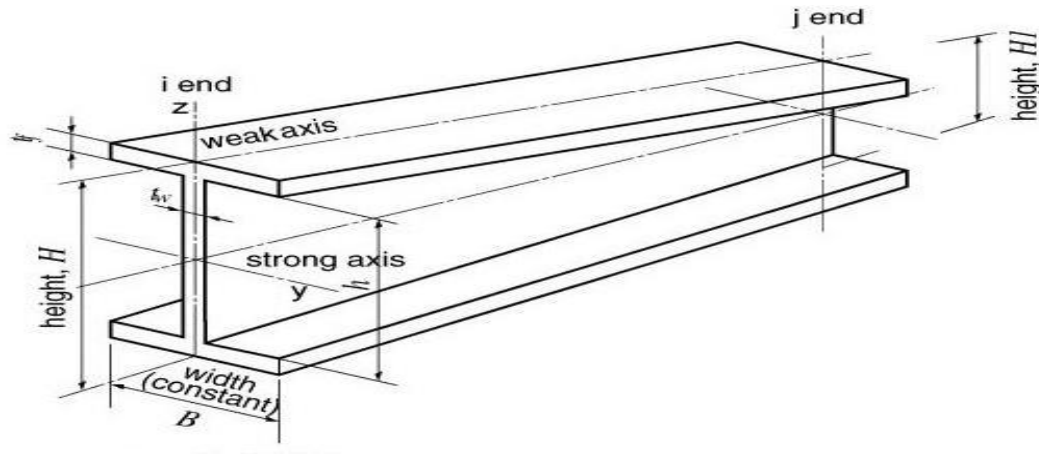


Figure 1.1 : Geometry of Typical Web Tapered I-Beam (Polyzois & Raftoyiannis, 1998)

Tapered beams are able to increase the stability of the structures and at the same time it is aesthetically pleasing which it could satisfy architectural demand. It could also satisfy functional requirements while reducing weight and cost in many fields of civil construction (Asgarian et al., 2013).

1.4 Perforation in Steel Section

There are several advantages of using perforated steel section. One of it is that it eases the integration of M&E services such as ventilation pipes and electrical cables within the structural depths of the beam. This will increase the ceiling to floor height as compared to the conventional plain webbed beam usage where the services pass underneath the beam (Tsavdaridis, 2012).

Perforation could also reduce the volume of material that is required without compromising too much on the structural strength or serviceability requirements. It could also alleviate the beam column joints from high stresses. Provision of openings in the beams is also aesthetically pleasing and could satisfy architectural needs (Lagaros et al., 2008). Perforation in the beams could be in a variety of shapes. The most commonly used shapes are circular, square, hexagon, diamond and octagon (Hasan et al., 2017). Figure 1.2 shows some of the shapes commonly used.

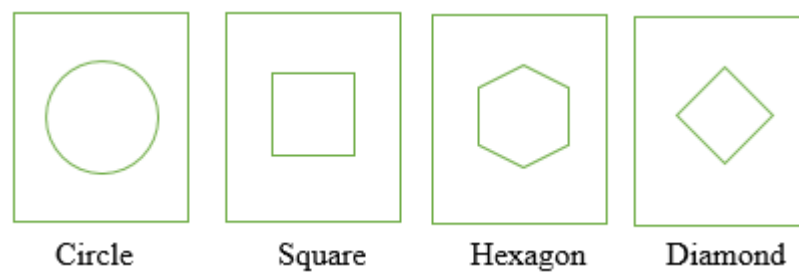


Figure 1.2 : Shapes of perforation (Hasan et al., 2017)

1.5 Problem Statement

Buckling moment capacities of tapered steel section with perforation decreases when the number of opening and opening size increases. The buckling moment capacity decreases when the ratio of tapering increases. From the research done by Azar et al. (2015), it only takes into account the buckling load that will cause the failure but not the self-weight of the material. Therefore, the effect of size and shape of perforation, opening layout, tapering ratio and flange and web thickness to the structural efficiency of the tapered steel section with perforation under lateral torsional buckling behaviour need to be studied. The self-weight of the tapered steel section with perforation also needs to be taken into account in order to determine the most efficient structure. The price of steel had surge tremendously due to the increased demand from the construction sector.

Therefore, it is essential to design structural element to be the most efficient to save material and cost.

The failure pattern of tapered steel section with perforation and tapered steel section without perforation does not have large dissimilarities (Azar et al., 2015). However, the failure pattern of the most efficient section has not been studied by any researchers previously. It is important for engineers to know where the stress will be concentrated when designing the most efficient tapered steel section with perforation. Therefore, it is important to study the failure pattern and stress distribution of the most efficient section to compare with the results obtained by Azar et al. (2015) to determine if there are any major difference.

1.6 Objectives

The objectives of this study are as follows:

1. to determine the effect of opening size, opening shape and opening layout of perforation to the efficiency of tapered steel section with perforation.
2. to determine the effect of tapering ratio and flange and web thickness to the efficiency of tapered steel section with perforation.
3. to determine whether the failure pattern and stress distribution of the most efficient tapered steel section with perforation has any major difference with typical tapered steel section with perforation to lateral torsional buckling.

1.7 Scope of study

The scope of the study involves:

1. The sectional properties of the model and length of the span is fixed in this study.
The depth, h of the tapered beam is 500mm at the fixed end and width, b is 250mm. The flange thickness ranges from 10mm to 20mm while web thickness ranges from 6mm to 15mm. The length of the span is fixed at 5.5m.
2. This study is only takes into account web tapered beam. Only one finite element software, LUSAS is used to analyse the model in this study.
3. The opening size of the perforation is limited from $0.3D$ to $0.75D$ only. Opening shape investigated in this study is limited to circular shape, square shape and diamond shape only.
4. Opening layout investigated in this study is limited to Open-Open-Open (OOO) layout, Open-Close-Open (OCO) layout and Close-Open-Close (COC) layout only. The tapering ratio is also limited from 0.3 to 0.75 only.

CHAPTER 2

LITERATURE REVIEW

2.1 Tapered Steel Section

Polyzois and Raftoyiannis (1998) carried out research on lateral torsional stability of steel web-tapered I-beams. In this research, finite element analysis for steel web-tapered I-beams is conducted and compared to the ones proposed by the current specifications. The current design specifications for steel tapered beams are re-examined while certain modifications are being proposed that covers a wider range of geometry and loading cases. Six specific cases of loading and restraining conditions are presented. Based on the results obtained from finite element analysis, separate expressions for the stress gradient factor B and the restraint factor R were developed and some recommendations for design considerations were proposed.

Andrade and Camotim (2005) carried out research on lateral torsional buckling of singly symmetric tapered beams: Theory and Applications. In this research, a general variational formulation to analyse the elastic lateral-torsional buckling (LTB) behaviour of singly symmetric thin-walled tapered beams is presented, numerically implemented, validated and illustrated. In this paper also shows that modelling tapered beam as an assembly of prismatic beam segments may lead to inaccurate results as it is conceptually inconsistent. Besides that the authors also demonstrated that the LTB behaviours of prismatic and tapered beams are qualitatively different. There are some simplifying assumptions made which are as follow:

1. Display thin-walled open cross sections
2. Singly symmetric (cross-section minor axes lying on the beam symmetry plane)
3. Made of homogenous, elastic and isotropic materials
4. Contain no initial imperfection

Asgarian et al. (2013) carried out research on lateral torsional buckling of tapered thin-walled beams with arbitrary cross-sections. In this paper, a theoretical and numerical model based on the power series method was investigated for the lateral buckling stability of tapered thin-walled beams with arbitrary cross-sections and boundary conditions. A number of numerical examples of tapered thin-walled beams were presented to determine the efficiency and accuracy of the method. The results obtained are also used to compare with finite element solutions using ANSYS software. Six comparative examples are studied in order to investigate the accuracy and efficiency of the power series method used for tapered thin-walled beams with arbitrary cross sections and boundary conditions in lateral buckling stability. In the first example, the lateral buckling stability of a tapered cantilever beam under a top flange tip load is being investigated. Two cross sections which are doubly I-section and singly symmetric I section are considered for the analysis.

Table 2.1 : I-cantilever web tapered beam (Asgarian et al., 2013)

L (m)	α	Lateral torsional buckling loads (kN)					
		Equal flanges			Unequal flanges		
		P_{cr} (ANSYS)	P_{cr}	Difference (%)	P_{cr} (ANSYS)	P_{cr}	Difference (%)
2	0.5	151.44	158.63	4.75	70.175	79.32	13.0
	1	166.45	169.05	1.56	71.271	78.788	10.6
4	0.5	42.121	43.16	2.47	25.64	25.84	0.78
	1	41.695	42.93	2.96	18.488	18.793	1.65
6	0.5	21.984	22.87	4.03	14.724	15.16	2.96
	1	18.544	18.138	2.19	9.736	9.687	0.50
8	0.5	13.681	14.25	4.16	9.534	9.72	1.95
	1	10.577	10.567	0.09	6.306	6.301	0.08
10	0.5	9.18	9.22	0.44	6.536	6.71	2.66
	1	7.147	7.116	0.43	4.529	4.544	0.33

From the results shown in Table 2.1, it is shown that the error percentage is high for short beam ($L=2m$). L in the table represents the length of the span of the beam while α represents tapering ratio of the beam. P_{cr} is the lateral torsional buckling loads which is the maximum load that the beam can resist before it fails due to lateral torsional buckling. For this case, the presence of local and overall buckling is always observed and therefore beam results for short beam lengths are questionable. The lateral-torsional buckling loads are higher for doubly I-section which has equal flanges compared to singly symmetric I section. It is shown that for web tapered beam with length equal to 4m or more, the lateral

torsional buckling loads increases when the tapering ratio decreases. The lateral torsional buckling behaviour of doubly symmetric and singly symmetric simply supported beams under a distributed load is investigated.

Table 2.2 : Simply supported web tapered I-section under distributed load (Asgarian et al., 2013)

L (m)	α	Lateral buckling moments (kNm), load on shear center					
		Doubly symmetric section			Singly symmetric section		
		FEM ANSYS	Calculation	Difference (%)	FEM ANSYS	Calculation	Difference (%)
6	0.6	79.64	79.26	0.48	60.23	59.466	1.27
	0.8	85.21	86.54	1.56	65.85	63.26	3.93
	1.0	92.32	93.82	1.62	66.23	67.44	1.83
8	0.6	57.86	57.14	1.24	43.368	42.266	2.54
	0.8	60.65	60.78	0.21	43.296	44.39	2.53
	1.0	63.9	64.465	0.88	46.34	46.811	1.02
10	0.6	45.46	44.67	1.74	32.21	32.78	1.77
	0.8	47.07	47.021	0.10	34.83	34.27	1.60
	1.0	48.98	49.226	0.50	35.47	35.71	0.68

From Table 2.2, the lateral buckling moments gradually decreases as the tapering ratio reduces. Besides that, lateral buckling moments increases with the decrease in span length. Doubly symmetric section also has a higher lateral buckling moment compared to singly symmetric section.

Marques (2012) carried out research on flexural and lateral torsional buckling on tapered steel members. The research focus to develop new stability rules for lateral and lateral torsional buckling of web-tapered members in which the buckling phenomena is accounted for by a proper buckling coefficient related to realistic imperfections. The objective was to have a straight forward procedure to design tapered members nevertheless with mechanical consistency. In this research, it is found out that it is noticeable that both the resistance and the plateau length increases with the increase of tapering. This increase is less significant for higher taper ratios. The influence of the tapering factor $\beta(x_c^{\text{II}})$ is also visible when comparing $\gamma_h=1$ (prismatic beam) with other values of γ_h .

Steel web tapered tee-section beams are widely used because it is aesthetically pleasing and light weight. These beams have low weight-to-strength ratios which is very good and are mostly cantilevered. They also have a high structural efficiency since the web is tapered to closely match the variation of bending moment along the beam. Therefore, the depth of the beam is largest at the fixed support as this is the location where the bending moment is the greatest. The depth of the beam will gradually decrease towards the free end (Yuan et al., 2013).

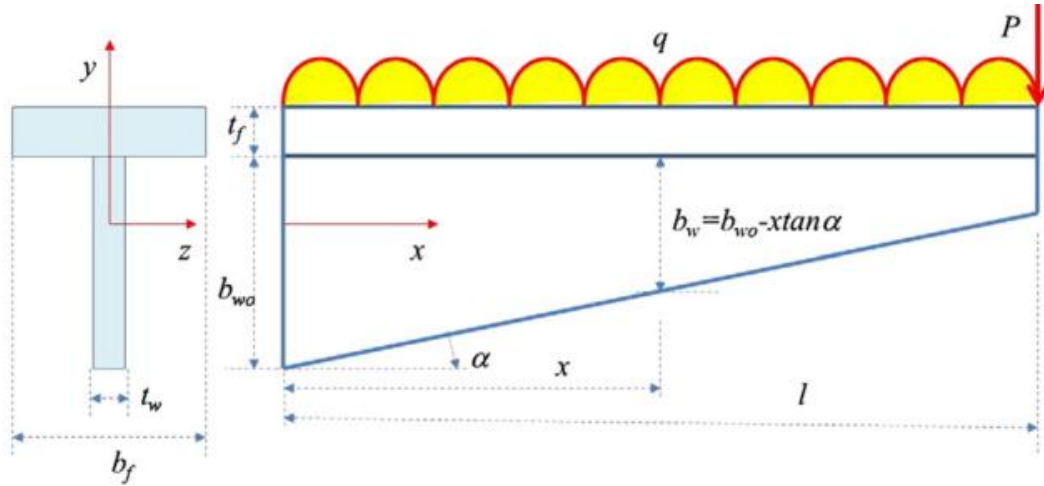


Figure 2.1 : A web tapered tee-section cantilever beam subject to a uniformly distributed load and a concentrated load at its free end (Yuan et al., 2013)

Yuan et al. (2013) carried out research with the topic of lateral torsional buckling of steel web tapered tee-section cantilevers. ANSYS software was used to simulate the lateral-torsional buckling behaviour of steel web tapered tee-section cantilevers. It is found that the critical buckling loads of the tapered beams could be higher or lower compared to the uniform tee-section beams. For beam with narrow flange (width/depth = 0.19), tapering reduces the buckling load up to 10% and 6% for the tip point loading and the uniformly distributed load respectively. On the other hand, for beam with a relatively wide flange (width/depth = 0.96), tapering increases the buckling load by 2%. Beam length could also affect the buckling load. When lateral torsional buckling occurs, the critical bending moment at the fixed support decreases with the increase of the beam length. The decrease rate is slightly quicker in the with a tip point load than in the beam with uniformly distributed load.

Trahair (2014) conducted a research on the interaction buckling of tapered beams. Research is carried out on two types of tapered beam which are tapered braced beams

and tapered continuous beams. It is found that there are three main factors that will affect the buckling of tapered beams. The factors are:

1. Effects of moment distribution
2. Effects of taper
3. Effects of end restraint

The effects of lateral buckling of a web-tapered beam without end restraints ($k=1$) can be determined from the equations below:

$$C_{bt} = M_t / (C_{bm} M_u) \quad (2.1)$$

where M_t is the maximum moment in a simply supported tapered segment. Taper effects for linearly web tapered segments may conveniently be allowed for by multiplying the classic lateral buckling moments, $C_{bm} \cdot M_u$ is computed using the mid-segment section properties by taper factors, C_{bt} . From the research by Trahair (2014), the values of C_{bt} had been determined for a number of different segment moment distributions using the computer program FTBTM. It is found that the differences of these with the degree of taper is small, compared to those based on the use of the properties of the smallest section. Therefore, tapering steel section will have an effect on the interaction buckling of beams.

2.2 Perforated Steel Section

Chung et al. (2001) carried out research with the title of investigation of Vierendeel mechanism in steel beams with circular web openings. The load carrying capacities of the beams is assumed to be limited by the formation of plastic hinges at the top tee-sections at the low moment side of the web opening. However, this is a very conservative

method since the formation of plastic hinges in the top tee-sections at the low moment side of the web openings does not always cause failure. The beam is still capable in carrying additional load until four plastic hinges at critical locations of the perforated sections are developed to form a Vierendeel mechanism. From the research done by Chung et al. (2001), the Vierendeel mechanism in steel beams with circular web openings is investigated based on analytical and numerical studies. The presence of web openings in steel beams introduces three different modes of failure at the perforated sections:

- Shear failure due to reduced shear capacity
- Flexural failure due to reduced moment capacity
- The ‘Vierendeel’ mechanism due to the formation of four plastic hinges in the tee-sections above and below the web openings under the Vierendeel action

In Chung et al. (2001) research, all hot rolled steel I-sections are of class 1 or 2 (plastic or compact). All the web openings are concentric to the mid-height of the sections with diameters between $0.5h$ and $0.75h$, where h is the depth of the sections. It is found that the load carrying capacities of steel beams with circular web openings obtained from the results of the finite element modelling are 5-10% higher than those obtained from the current design method based on the formation of LMS plastic hinges. The reduction in shear capacity of the perforated section is found to be more critical than the reduction in moment capacity for steel beams with circular web openings. Besides that, it is also found that the effect of structural performance due to the presence of web openings may be eliminated completely through rational design of the web openings in terms of the locations along beam span and also the size of opening.

Lagoros et al. (2008) carried out research on optimum design of steel structures with web openings. The main objective of this paper is to perform optimum design of 3D steel structures with perforated I-section beams. The sizing design variables are the cross-sectional dimensions of the columns and beams while the topology and shape design variables are the number and size of the web openings of the beams. According to Chung and Lawson (2001) covering composite beam with large web openings, there are certain restrictions that have to be followed:

1. All web openings should be located along the centreline of the web. This is because generally shear force is resisted by upper section of web-flange while lower web-flange is often highly stressed in tension due to bending moment and therefore considerable deviation from the centre line would causes failure of the smaller tee section.
2. The maximum diameter of circular opening should not exceed 0.75 times the total height of the beam. This is because an extremely large opening will cause the shear and moment capacities to be reduced.
3. The distance between the edges of adjacent openings should not be less than the total height of the beam. This is because adjacent openings that are too close may induce web buckling phenomena.

From the study by Lagoros et al. (2008), five test cases have been examined. The first one corresponded to the beam element discretization while the remaining four to the shell element discretization with and without web openings. The two formulations which are beam element and shell element discretization are compared in terms of the optimum designs achieved. A characteristics test example considered in the study by Lagoros et al. (2008) showed that by allowing web openings in the beams of the structure, a

quantifiable reduction in the weight of the structure is accomplished and at the same time without reducing structural strength or serviceability requirements.

Ellobody (2012) carried out research on nonlinear analysis of cellular steel beams under combined buckling modes. A nonlinear 3-D finite element model has been developed which accounts for the initial geometric imperfection, residual stresses and material nonlinearities of flange and web portions of cellular steel beams. Finite element analysis software, Abaqus is used to predict the failure loads, load-mid-span deflection relationships and failure modes of cellular steel beams. A total of 120 cellular steel beams were analysed using the verified finite element model to determine the effect of cross-section geometries, beam length and steel strength on the strength and buckling behaviour of cellular steel beams. The results show that cellular steel beams failing due to combined web distortional and web-post buckling modes have exhibited a considerable decrease in the failure loads. The use of high strength steel will also increase failure loads of less slender cellular steel beams. The failure loads predicted from the finite element model were compared with that predicted from Australian Standards for steel beams under lateral torsional buckling. The results show that Australian Standards predictions for normal strength and high strength cellular steel beams failing by lateral torsional buckling is conservative while it is unconservative for cellular steel beams failing by combined web distortional and web-post buckling.

Tsavdaridis and D'Mello (2012) carried out research on the topic of optimisation of novel elliptically-based web opening shapes of perforated steel beams. The objective of this research is to investigate the behaviour of perforated steel beams with different novel web opening shapes. Shapes are also optimised for beams that are subjected to high shear

forces. From the research by Tsavdaridis and D'Mello (2012), the author found out that all perforated beams with the novel elliptically-based web opening shapes ($d_o=0.8h$) are stiffer compared to the perforated beams with circular web openings (either $d_o=0.8h$ or $d_o=0.76h$). Vertical deflections of the novel specimens are also smaller. All perforated beams with novel elliptical web openings ($d_o=0.8h$) present increased stiffness, mainly in the plastic region. Their maximum vertical deflections are even lower than perforated beams with circular web openings with a smaller diameter ($d_o=0.76h$). Besides that, it also found that there are two factors that affect the stresses in the vicinity of the web openings which are θ and R . However, the deflections of the perforated beams are only affected by radius, R as it is the main parameter which determines the web opening area and the critical opening length, c at the top and bottom tee-sections.

Rodrigues et al. (2014) carried out a research with the topic finite element modelling of steel beams with web openings. This paper presented finite element models to investigate structural response of steel beams with web openings in terms of stress distribution, collapse load magnitude and associated failure modes using ANSYS software. The objective of this research is to determine the most efficient shape, size and location of the openings. The study also investigated the efficiency of longitudinal stiffeners welded at the opening region and benefits of using an adequate edge concordance radius in beams with rectangular and square openings. Figure 2.2 shows the three local actions induced at the upper and lower “Tees” present in a perforated section subjected to global bending moment and a shear force.

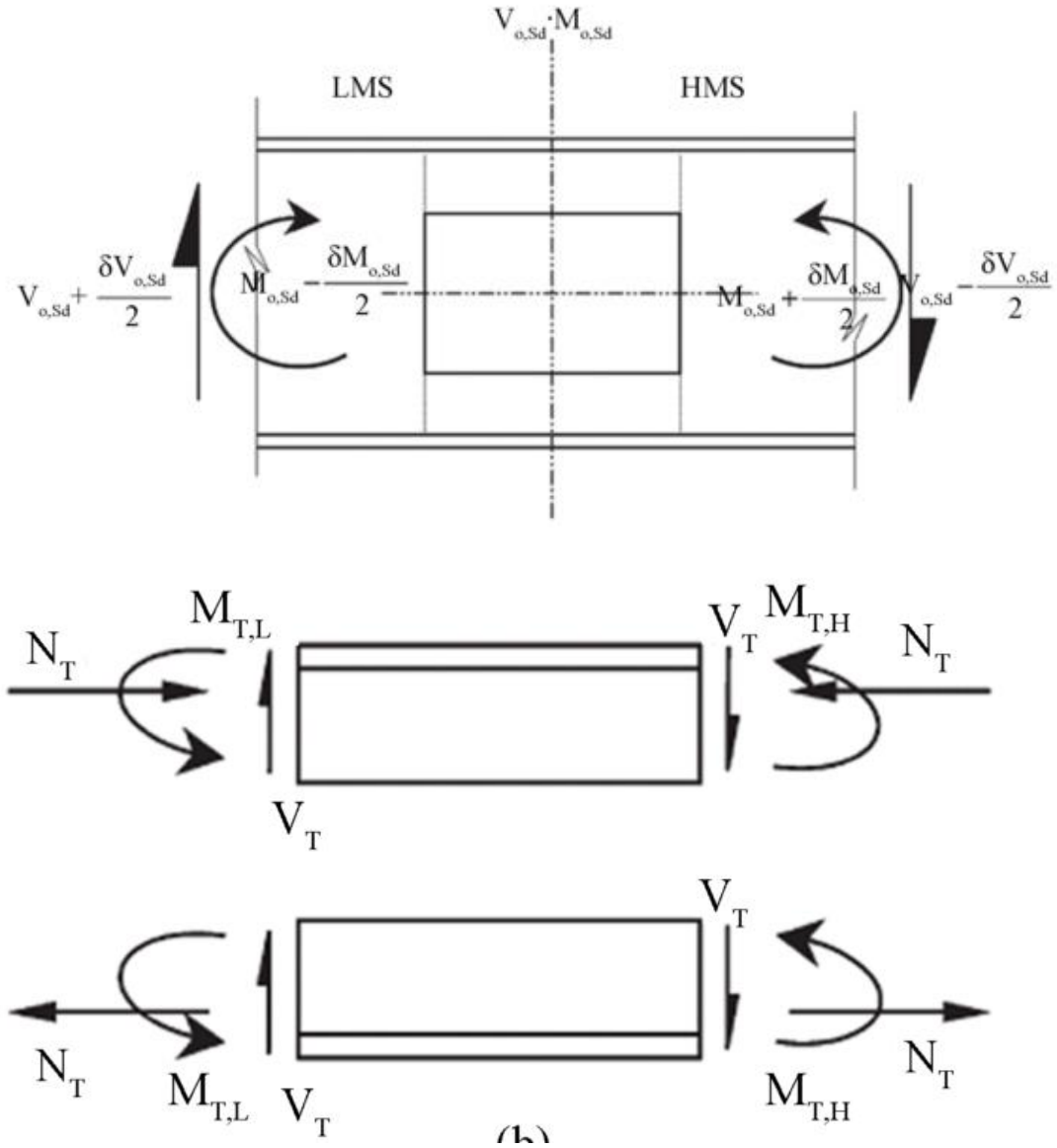


Figure 2.2 : Perforated section force distribution (Rodrigues et al., 2014)

The results from the finite element simulations was calibrated against numerical and test results to validate the results obtained from the finite element. The results from this research indicated that opening geometry influences the steel beams load carrying capacity significantly. Beams with rectangular openings has smaller ultimate loads which is around 30% less than beams with square or circular openings. From the results, it was observed that the beam with circular opening presented an ultimate load five and two and a half times the ultimate load associate to beams with rectangular and square openings respectively. This could be due to the better stress redistribution achieved with the

circular opening configuration that led reduction on the stress concentration at the beam web opening edge region.

2.3 Structural Efficiency

Hasan et al. (2017) carried out research with the topic of the efficiency of I-beam steel section with perforated-corrugated web profile. The objective of this research is to determine the structural efficiency of the Triangular Web Profile (TriWP) with perforated web caused by various combinations of shapes, sizes and the layouts of perforations. Besides that, the author also wants to investigate the effect of section properties and span length on the structural behaviour of Triangulated Web Profile with perforated web. A total of 359 models of TriWP with and without perforation have been investigated in this study. The self-weight of the models are calculated beforehand.

Table 2.3 : Self-weight of TriWP with perforation for Layout 3 (Hasan et al., 2017)

Perforation Size	Selfweight (kN)				
	TriWP with perforation				
	Circle	Square	Hexagon	Diamond	Octagon
0.4D	0.1553	0.1537	0.1556	0.1576	0.1560
0.5D	0.1519	0.1492	0.1523	0.1554	0.1528
0.6D	0.1476	0.1438	0.1482	0.1527	0.1490

From Table 2.3, the self-weight of TriWP with square opening is the lowest as compared to circle, hexagon, diamond and octagon of the same perforation size. This is because square has the largest area of opening compared to other shapes.

Table 2.4 : Percentage difference of weight reduction of TriWP with perforation for Layout 3 (Hasan et al., 2017)

Perforation Size	Percentage of weight reduction (%)				
	TriWP with perforation				
	Circle	Square	Hexagon	Diamond	Octagon
0.4D	3.86	4.91	3.69	2.47	3.48
0.5D	6.02	7.66	5.75	3.84	5.42
0.6D	8.65	11.01	8.26	5.52	7.79

From Table 2.4, percentage difference of weight reduction for TriWP with square perforation shape and without perforation is also the highest compared to other shapes with the same perforation size. The percentage of weight reduction also increases when the perforation size increases from 0.4D to 0.6D as the web opening size increases.

Finite element analysis was then used to analyse the TriWP with and without perforation to four types of loading condition which are bending, lateral torsional buckling, torsion and shear deformation. In the lateral torsional buckling loading conditions, Layout 3 with diamond perforation shape and 0.4D perforation size shows the highest buckling load compared to other layout. This is because Layout 3 has the least number of openings. Diamond perforation size also shows the least weight reduction. Smaller perforation size also results in higher buckling load.

Table 2.5 : Buckling load of TriWP with perforation (Hasan et al., 2017)

Perforatio n Shape	Buckling Load, P _b (kN)								
	Layout 1			Layout 2			Layout 3		
	0.4D	0.5D	0.6D	0.4D	0.5D	0.6D	0.4D	0.5D	0.6D
Circle	97.75	91.8	86.02	97.74	91.77	86.6	122.4	107.5	101.8
		7				0	2	4	0
Square	92.88	84.1	73.78	92.78	82.68	75.5	105.6	105.9	105.3
		4				0	5	0	8
Hexagon	97.72	91.8	84.88	115.0	91.69	85.3	105.4	105.3	105.1
		7		3		2	1	0	1
Diamond	100.6	97.4	110.3	118.4	114.7	93.9	125.9	121.1	109.1
	6	1	2	6	7	6	2	7	8
Octagon	96.37	89.7	82.34	96.44	89.69	82.7	105.4	105.2	105.7
		0				6	9	2	8

The structural efficiency of all models are then calculated using the equation below:

$$\text{Structural efficiency} = \text{Buckling moment} / \text{Self-weight} \quad (2.2)$$

From Table 2.5, the highest buckling load is 125.92 for TriWP with Layout 3 which has diamond perforation shape and perforation size of 0.4D. This is because it has the least number of opening with the smallest opening area and therefore it is able to resist a higher buckling load.

Table 2.6 : Structural efficiency of TriWP with perforation (Hasan et al., 2017)

Perforation Shape	Structural Efficiency								
	Layout 1			Layout 2			Layout 3		
	0.4D	0.5D	0.6D	0.4D	0.5D	0.6D	0.4D	0.5D	0.6D
Circle	662.3	657.1	660.7	635.5	614.3	600.9	788.3	797.7	689.7
Square	645.9	628.8	606.7	615.0	565.9	541.6	687.4	709.8	732.8
Hexagon	659.4	652.5	645.0	746.4	611.3	588.8	677.4	691.4	709.2
Diamond	659.2	659.5	779.1	756.5	746.2	624.3	799.0	692.0	715.0
Octagon	647.2	632.0	617.7	623.8	595.6	567.2	676.2	688.6	667.8

The percentage difference of structural efficiency is calculated using the equation below:

$$\% \text{ of structural efficiency} = [(a - b / a)] \times 100\% \quad (2.3)$$

From Table 2.6, the highest structural efficiency obtained is 799.0 for TriWP with Layout 3 which has diamond perforation shape and perforation size of 0.4D. The second highest structural efficiency is 797.7 for TriWP with Layout 3 which has circle perforation shape and perforation size of 0.5D. The lowest percentage difference of structural efficiency is 2.0% for TriWP with Layout 3 with diamond perforation shape and 0.4D perforation size. This means that it can perform almost as well as TriWP without perforation to lateral torsional buckling.

In Stage 2 of the study, TriWP with Layout 3 with diamond perforation shape and 0.4D perforation size was selected to determine the effect of flange thickness, web thickness and span length. The results showed that when the span length of the model increases, the buckling moment resistance decreases. Meanwhile, the buckling moment resistance

increases when the flange thickness and web thickness increases under the same span length.

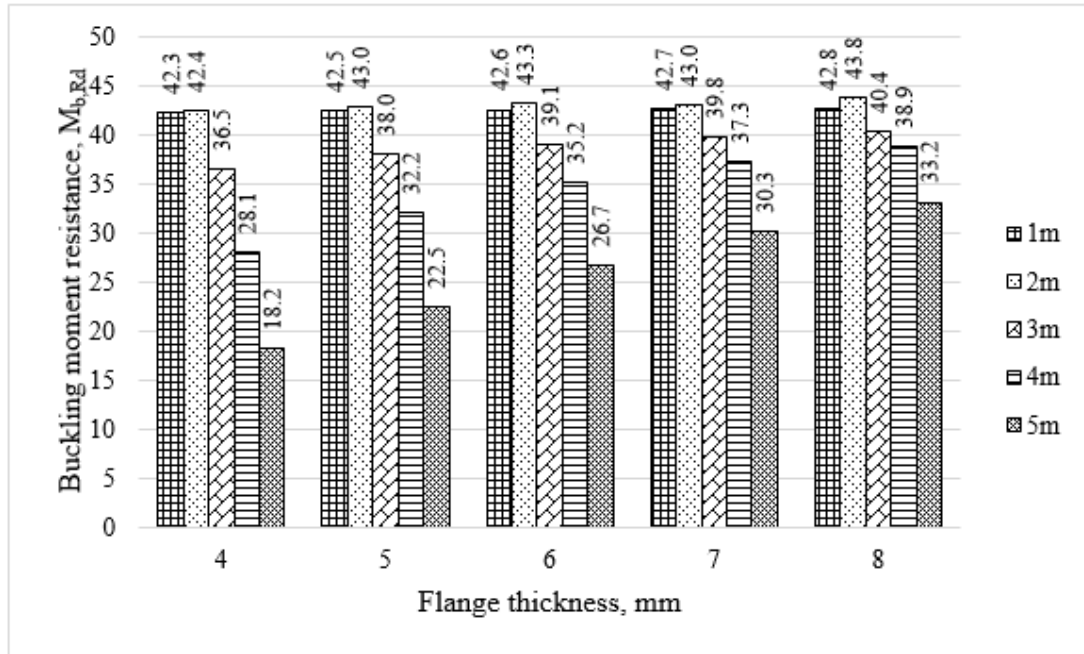


Figure 2.3 : Buckling moment resistance versus flange thickness for TriWP with diamond perforation shape and perforation size of 0.4D in Layout 3 (Hasan et al., 2017)

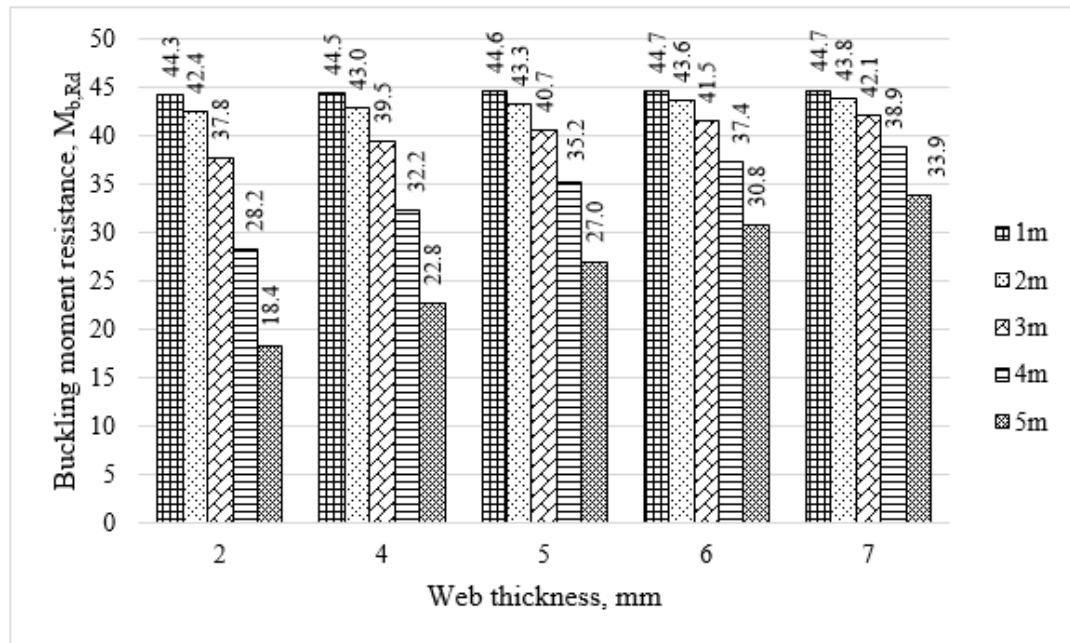


Figure 2.4 : Buckling moment resistance versus web thickness for TriWP with diamond perforation shape and perforation size of 0.4D in Layout 3 (Hasan et al., 2017)

From Figure 2.3, it is found that under the same web thickness the buckling moment resistance is found to increase when the flange thickness is increased. When the length of the model increases, the buckling moment resistance decreases as well. Flange thickness of 8mm with 2m span of beam shows the highest buckling moment resistance of 43.8 while flange thickness of 4mm with 5m span of beam shows the lowest buckling moment of resistance of 18.2. This is because thicker flange would be able to contribute in resisting lateral torsional buckling. Under the same flange thickness, the buckling moment resistance increases as the web thickness increases as shown in Figure 2.4. From Figure 2.4, both web thickness of 6mm and 7mm with 1m span of beam has the highest buckling moment resistance of 44.7. Therefore, by increasing the flange and web thickness, the buckling moment resistance increases under the same span length. Buckling moment resistance will also reduce when the span length increases.

2.4 Lateral Torsional Buckling

Benyamina et al. (2013) carried out research on analytical solutions attempt for lateral torsional buckling of doubly symmetric web-tapered I-beams. Firstly, the elastic equilibrium governing equations are carried out from the stationary condition. Secondly, the Ritz's method is deployed in order to derive the algebraic equilibrium equations. An analytical formula is proposed for the lateral buckling strength of web tapered beams in function of the classical stiffness terms, the load height position and the tapering parameter. The proposed formula is simple and could produce accurate results when compared to finite element simulations.